Check for updates

DOI: 10.1111/jiec.13219

RESEARCH AND ANALYSIS

JOURNAL OF INDUSTRIAL ECOLOGY WILEY

Simultaneously tracing the fate of seven metals at a global level with MaTrace-multi

Christoph Helbig[1] | Yasushi Kondo[2] | Shinichiro Nakamura[2]

[1] Resource Lab, University of Augsburg, Augsburg, Germany

[2] Faculty of Political Science and Economics, Waseda University, Shinjuku-ku, Tokyo, Japan

Correspondence
Christoph Helbig, Resource Lab, University of Augsburg, Universitätsstraße 16 , 86159 Augsburg, Germany.
Email: christoph.helbig@wiwi.uni-augsburg.de

Editor Managing Review: Ichiro Daigo

Funding information
C.H. was supported for this work by the Japan Society for the Promotion of Science (JSPS) under the program "FY2019 JSPS Postdoctoral Fellowship for Research in Japan (short-term)" with Grant No. PE19729. Y.K. and S.N. were supported by JSPS KAKENHI Grant Number JP19H04328.

[The copyright line for this article was changed on 24 January 2022 after original online publication.]

Abstract

Keeping materials in use for a long time is key to reducing primary material demand and environmental impacts of resource use. Recycling yields of metals should only be limited by thermodynamically unavoidable losses of the remelting processes for well-defined scraps. In practice, however, additional dissipative losses for metals occur due to incomplete collection of end-of-life products, insufficient waste sorting, remelting of contaminated or diluted scrap, and the downcycling of secondary materials. Here we simultaneously trace the fate of Al, Cr, Fe, Ni, Cu, Zn, and Pb in MaTrace-multi, a planetary dynamic material flow system. Metals pass the processes mining, fabrication, use-phase, collection, sorting, scrap allocation, remelting, and secondary material allocation. We calculate the circularity and longevity of the cohort of metal requirements for the final demand of 1 year. Nickel is found to have the best longevity at 116 (78 to 205) years, whereas zinc only has a longevity of 47 (37 to 61) years. While nickel, on average, is used in 5.13 (3.45 to 8.78) applications before dissipation, zinc is used only in 1.94 (1.52 to 2.47) applications. Our study results can be used to model the impacts of circular economy policies and technological developments on global metal cycles beyond the scope of studies modeling one metal at a time. This article met the requirements for a Gold–Gold *JIE* data openness badge described at http://jie.click/badges

KEYWORDS
circular economy, dissipative losses, industrial ecology, material flow analysis, metals, recycling

1 | INTRODUCTION

In 2018, greenhouse gas emissions of 4.6 $GtCO_2e$ were directly or indirectly caused by metal production, equal to 7.9% of the annual global emissions (Lamb et al., 2021). Implementing a circular economy for metals is key to reducing the required global primary material production and greenhouse gas emissions linked to metal production (Watari et al., 2020). Mining needs should be limited to replacing thermodynamically unavoidable losses and expanding in-use stocks of metals (Jelinski et al., 1992). Metals are often said to be ideal materials for the circular economy because they are very well recyclable. Metals are not destroyed in their use-phase, and usually, there are recycling processes available. In practice, however, many

This is an open access article under the terms of the Creative Commons Attribution-NonCommercial License, which permits use, distribution and reproduction in any medium, provided the original work is properly cited and is not used for commercial purposes.
© 2022 The Authors. *Journal of Industrial Ecology* published by Wiley Periodicals LLC on behalf of the International Society for Industrial Ecology.

metals show low recycling rates (Graedel et al., 2011). The only cases where metals become intentionally unrecoverable are dissipative uses (Ciacci et al., 2015). Increasing the recovery rates of metals would, for many metals, reduce the related GHG emissions by reducing primary production requirements, and also due to the lower emission factors of secondary production compared to primary metal production (Nuss & Eckelman, 2014; Van der Voet et al., 2019). To identify opportunities for increased recovery rates, we need to quantify how metals behave in the anthroposphere and identify the hotspots for metal losses (Izatt et al., 2014; Reck & Graedel, 2012). Ultimately, metals will be lost from the global cycles through some form of dissipation, meaning they become technically or economically unrecoverable (Zimmermann & Gößling-Reisemann, 2013).

Material flow analysis (MFA) is a standard industrial ecology method to describe these metal cycles (Brunner & Rechberger, 2016). Dynamic MFA can be used, for example, to analyze stock dynamics in the past and present (Krausmann et al., 2017) or to quantify the evolution of material-related environmental impacts (Watari et al., 2020). In the past, metal cycles have often been assessed one metal at a time (Chen & Graedel, 2012; Graedel, 2019; Müller et al., 2014). For all the metals evaluated in this article, individual cycles have been developed: aluminum (Bertram et al., 2017; Cullen & Allwood, 2013), chromium (Johnson et al., 2006), iron or steel (Cullen et al., 2012; Wang et al., 2007), nickel (Reck et al., 2008; Reck & Rotter, 2012), copper (Ayres et al., 2002; Glöser et al., 2013), zinc (Graedel et al., 2005; Meylan & Reck, 2017), and lead (Mao et al., 2008a, 2008b). However, it has been noted that future models need to address the challenges of the circular economy in terms of product- and material-specific answers. They need to include the reality that metal cycles are interlinked (Reuter et al., 2005). The mixing of metals in products, either by design or through unintended contamination, thermodynamically complicates the recovery of metals (Reuter & Kojo, 2012). Simultaneous modeling of multiple metals is helpful because it allows considering thermodynamics in the remelting processes (Reuter et al., 2018, 2019). For example, for most alloying metals in aluminum scrap, separation during aluminum remelting is hampered by the high reactivity (a high affinity for oxygen) of aluminum (Nakajima et al., 2010). This high reactivity of aluminum and the generally higher tolerance for alloying elements in cast aluminum alloys leads to the observed downcycling from wrought to cast aluminum (Cullen & Allwood, 2013). As a second example, contamination of steel scrap with copper should be evaluated differently because a copper content above a threshold limits use to reinforcing bars (Daehn et al., 2017). Zinc, in turn, is typically removed from steel in the Waelz kiln process because of its high vapor pressure and is consequently supplied to a zinc refinery (Nakajima et al., 2008). Suppose the contaminating substances are persistent and hazardous, like cadmium. In that case, this additionally implies a policy conflict between resource circulation on the one hand and environmental and health regulations on the other (Johansson & Krook, 2021). These environmental and health considerations of metals may even affect non-metal flows and stocks, such as food or plastics, which could also be assessed (Puype et al., 2015; Turner & Filella, 2017). Here, however, we focus on the flows of seven metals.

A suitable model to trace metals in the global economy is the so-called *MaTrace* model. In this context, *tracing* means identifying metals' fate within a specific cohort (e.g., the production within 1 year) throughout time. MaTrace has first been developed and applied to steel in Japan by Nakamura et al. (2014). In later updates, *MaTrace-global* identified steel and steel products' regional distribution through recycling (Pauliuk et al., 2017). *MaTrace-alloy* simultaneously identified the losses of Fe, Ni, and Cr in steel material cycles (Nakamura et al., 2017). Additionally, Helbig et al. (2020) have shown that the data of many single-metal mass balance models can be used in MaTrace-like stock and flow models to calculate dissipation ratios and expected lifetimes in the anthroposphere. MaTrace was recently applied to copper flows (Klose & Pauliuk, 2021) and cobalt (León et al., 2020).

Here, we show an extension of the *MaTrace* model to non-steel applications. The presented dynamic material flow model *MaTrace-multi* simultaneously traces the fate of seven major elements in the global economy, namely aluminum, chromium, iron, nickel, copper, zinc, and lead. We start with the metal requirements for the product cohort of the final demand in 1 year and trace the fate of this cohort through multiple open-loop cycles over a time frame of 1000 years. In the end, the in-use stock for all metals has been dissipated through one process or another. Over the evaluated period, yields and allocation parameters are held constant, allowing quantifying a "what-if" scenario: To estimate how long a metal cohort stays in the anthroposphere given the current state of global metal cycles. Phenomena of metal mixing in the waste management stages of all seven metals are visualized with Sankey diagrams. The phenomena are characterized by the simultaneous evolution of multiple metals interacting and mixing up together over cycles of sorting and metallurgical processes. Therefore, it is unavoidable that the mathematics involved is more complex than the one used in the standard MFA concerned with a single metal at a time. Still, we tried our best to minimize the complexity, say by reducing the extent of simultaneity, without sacrificing the essential feature of the model. In particular, this simplification applies to the treatment of process waste.

We identify the leading causes for material losses and quantify two indicators for the circular economy for each of the metals—circularity and longevity—as recently presented by Klose and Pauliuk (2021). *MaTrace-multi* is implemented using the open software framework for studying dynamic material systems (ODYM) developed by Pauliuk and Heeren (2020).

The method section describes the setup of the dynamic stock and flow model, its quantitative structure, and the calculation of the circularity and longevity indicators to analyze the metals' fate. The results section shows the quantitative results for the metals Al, Cr, Fe, Ni, Cu, Zn, and Pb.

2 | METHODS

In *MaTrace-multi*, consistent with the ODYM framework (Pauliuk & Heeren, 2020), metals, or chemical elements, cannot be altered because they are atoms. Mass conservation for all processes and metals is the fundamental modeling principle. The only exceptions for these fundamental

principles, nuclear reactions, and effects of relativity, are not relevant for the global cycles of any of the seven metals in this model. MaTrace-multi is a dynamic stock and flow model consisting of transformation and distribution processes, including stocks and flows linking the processes (Brunner & Rechberger, 2016). Inflows and outflows are linked through transfer coefficients, given as exogenous parameters. The change of stock within a process equals the difference between all inflows and all outflows. The fate throughout time is quantified for the cohort of metal content in durable products' global production within 1 year, depending on the product lifetime distributions and transfer coefficients.

2.1 | Material flow system

The material flow system of *MaTrace-multi* is described by its spatio-temporal boundary, the processes, and the considered metal flows (Brunner & Rechberger, 2016). We calculate 1000 years after the starting year for our fate modeling. Such an extended period is necessary to achieve convergent results for circularity and longevity. Figures on stock dynamics only display values for the first two centuries. *MaTrace-multi* is a global one-region model, meaning we do not consider trade as a dedicated distribution process. The system consists of the eight anthropogenic processes depicted in Figure 1 and the process-linking material flows and the exogenous parameters in each process. The processes are mining, fabrication, use-phase, collection, sorting, scrap allocation, remelting, material allocation, and the surrounding environment, which includes landfills.

The seven metals, identified with index *e* for element, are included in the form of products (*p*), scraps (*s*) or materials (*M*), except for the extraction of primary resources from the lithosphere as a subsystem of the environment, at which stage only elements are considered. We consider 11 product categories as durable products based on the classification of products in EXIOBASE3 (Stadler et al., 2018): beverages; chemicals; fabricated metal products; machinery and equipment; office and service industry machines; electrical machinery; radio, television, and communication devices; medical precision and optical instruments; motor vehicles; other transport equipment; and construction work. Product categories are relevant for the fabrication process, the product lifetime and in-use dissipation in the use-phase, and the collection process. For old scraps, we consider 12 scrap types: wrought and cast aluminum scrap; galvanized, carbon, other alloys, ferritic stainless, austenitic stainless, and Ni-alloy steel scrap; nickel scrap; copper scrap; zinc scrap; and lead scrap. Scrap types are relevant for the sorting process and the subsequent scrap allocation process. The scrap types in this study match those in relevant MFA studies and MaTrace-alloy with chromium being predominantly recycled through stainless steel scrap (Cullen & Allwood, 2013; Glöser et al., 2013; Johnson et al., 2006; Mao et al., 2008a; Meylan & Reck, 2017; Nakamura et al., 2017; Reck et al., 2008). Engineering materials, identified with index *M*, are either primary materials (*m*) produced through mining and quarrying or secondary materials (*n*) made from end-of-life scrap. In total, we consider 17 materials: 7 primary materials, which are identical to the 7 metals, and 10 secondary materials: wrought and cast aluminum; carbon, structural, ferritic stainless and austenitic stainless steel; nickel matte; secondary copper; secondary zinc; and secondary lead. This differentiation of primary and secondary materials is necessary because not all input–output tables used in

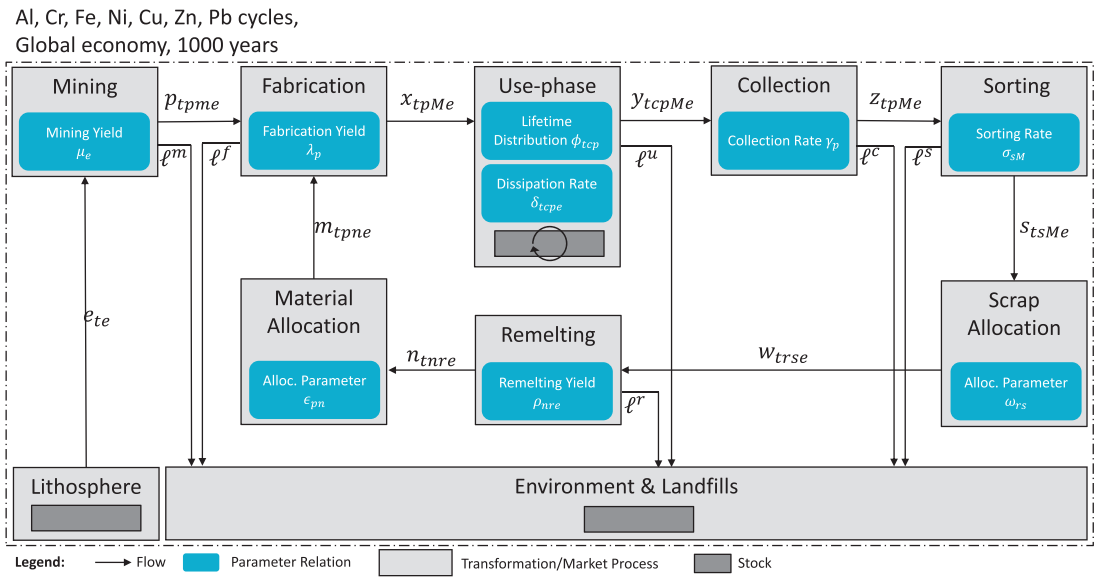

FIGURE 1 Processes and flows considered in MaTrace-multi. Flows: loss material flows *l* are dissipative losses; *e*, extraction; *p*, primary production; *x*, final production; *y*, end-of-life wastes; *z*, collected end-of-life wastes; *s*, sorted scrap; *w*, allocated scrap; *n*, remelted material; *m*, allocated secondary production. Parameters: μ, mining yield; λ, fabrication yield; ϕ, lifetime distribution; δ, in-use dissipation rate; *y*, collection rate; σ, sorting rate; ω, scrap allocation parameter; ρ, remelting yield; $\in$, material allocation parameter. Indices: *t*, time; *c*, cohort; *p*, end-use product; *M*, engineering material; *m*, primary material; *n*, secondary material; *s*, scrap; *r*, remelting process; *e*, element

our analysis differentiate between primary and secondary material flows. EXIOBASE3 lists both aluminum (products) and secondary aluminum for treatment (Stadler et al., 2018), but the Japanese input–output table lists aluminum including regenerated aluminum (Ohno et al., 2014). Therefore, the material composition of products could only be calculated on an element level. Materials are relevant in the remelting process, the subsequent material allocation process, and the sorting process. The 10 secondary materials correspond to the 10 considered remelting processes, which are following the relevant MFA studies and MaTrace-alloy (Cullen & Allwood, 2013; Glöser et al., 2013; Johnson et al., 2006; Mao et al., 2008a; Meylan & Reck, 2017; Nakamura et al., 2017; Reck et al., 2008). Products, scraps, and materials are chemically persistent if they are not processed further. However, products, scraps, and materials are, unlike elements, temporary and can be formed or destroyed by transformation processes. For example, the sorting process—which includes sorting, disassembly, and shredding—transforms engineering materials into scraps. Ten different considered remelting processes, identified with index *r*, transform scraps into secondary materials. We distinguish remelting and refining of aluminum; carbon, structural alloy, ferritic stainless, and austenitic stainless steel remelting; nickel matte remelting; copper remelting; zinc remelting; and lead remelting. Remelting processes may also have multiple secondary materials as output flows, including zinc recovery from electric arc furnace dust. Remelting processes are relevant for the scrap allocation process and the remelting itself. This way, the whole waste management and recycling sector is split into waste collection, scrap sorting, allocation of scraps to remelting processes, remelting of scraps to secondary materials, and allocating secondary materials to fabricated products.

2.2 | Calculation

MaTrace-multi, just as previous MaTrace models (Nakamura et al., 2014, 2017; Pauliuk et al., 2017), is initiated by tracing the material cohort for metals present in the final production x_{tpMe} at a specific time *t*. Such a cohort consequently gets index *c* equal to *t* for further identification. For the first period, an initial final production needs to be considered, which is modeled as consisting of only primary materials. Generally, we use global data for parameters required in MaTrace-multi but fall back to national data if the global data source does not provide us with the required level of detail. Therefore, the calculation of the final production of the initial time period uses data from EXIOBASE3 (Stadler et al., 2018) for the final demand of products in monetary units and data from Ohno et al. (2014) for chemical material composition of products calculated with waste input–output MFA (Nakamura et al., 2007).

Secondary materials are modeled only after the initial final production and are therefore not present in the initial period. In contrast to previous MaTrace models, MaTrace-multi also quantifies losses before the first use-phase (Helbig et al., 2020; Klose & Pauliuk, 2021; León et al., 2020; Nakamura et al., 2014, 2017; Pauliuk et al., 2017). There needs to be a primary fabrication stage to provide the metals required for the final products in the initial period. Primary materials p_{tpme} are fabricated into products with a product-specific fabrication yield λ_p. Due to data limitations, we assume that the fabrication yield does not depend on the material used in the fabrication process. Fabrication yields include internal reuse of recovered process wastes. The fabrication yield determines the fabrication stage losses from both primary and secondary production through mass balance. Metals e_{te} for primary fabrication are extracted from the lithosphere through mining and quarrying. Here, we only consider the metal content of these extraction flows. There are substantial non-metal material flows at the mine site level, like waste rock, which also pose environmental risks, but are outside the scope of our model (Lèbre et al., 2017). The metal-specific mining yield μ_e determines the losses in the mining stage through mass balance. The material flows of extracted metals are determined by the material composition of initial final products demanded, the fabrication yield, and the mining yield:

$$e_{te} = \mu_e^{-1} \sum_m \sum_p \lambda_p^{-1} x_{tpme}. \tag{1}$$

The products emerging from final production stay in the use-phase for the duration of their lifetime, modeled as a product-specific Weibull lifetime distribution ϕ_{tcp}, or until they are dissipated within the use-phase, modeled as a product- and element-specific exponential distribution δ_{tcpe}. All product lifetime distributions are assumed to be Weibull distributions with the three product-specific parameters: shape, scale, and location. Lifetime distribution parameters are modeled as constant throughout the years. All in-use dissipation exponential distribution rate parameters are determined by combining the average product lifetime with each element's in-use dissipation ratio estimated by Ciacci et al. (2015). End-of-life products y_{tcpMe} from different cohorts *c* are collected as wastes with a product-specific collection rate γ_p and from collected end-of-life wastes z_{tpMe}. Collection rates are typically low for small products or products with a low value but can be increased significantly, for example, with take-back systems. The collection rate determines the losses in the collection stage by mass balance. The material flows of collected end-of-life wastes are therefore determined by the material composition of final products, the lifetime distribution ϕ_{tcp}, which represents the fraction of product *p* from cohort *c* that is discarded during year *t*, in-use dissipation cumulative distribution function Δ_{tcpe} and the collection rate:

$$z_{tpMe} = \gamma_p \sum_{c=0}^{t-1} \phi_{tcp} \left(1 - \Delta_{tcpe}\right) x_{cpMe}. \tag{2}$$

Collected end-of-life product waste z_{tpMe} is sorted into scrap types, determined by a material-specific sorting ratio σ_{sM}. The sorting process is the first stage in waste management, where the mixing of materials and a gradual change of chemical composition may occur. The sorting ratio also determines the losses in the sorting stage by mass balance, which are relatively small, because only losses within waste separation and sorting are considered (collection losses are already considered before this process). Sorted scraps s_{tsMe} are allocated with an allocation parameter ω_{rs} to remelting processes, identified by index r, to recycle metals through the production of secondary materials. The scrap allocation is only a distribution process; no losses are considered at this stage. The material flows of scrap allocated to remelting processes are determined by the material composition of collected end-of-life wastes, the sorting ratio, and the scrap allocation parameters:

$$w_{trse} = \omega_{rs} \sum_{p} \sum_{M} \sigma_{sM} z_{tpMe}. \tag{3}$$

Metallurgical parameters determine the remelting yield ρ_{nre} of each metal in each remelting process. The remelting process is the second process where mixing and a gradual change of chemical composition may occur. The remelting yield determines the losses in the remelting stage by mass balance. Produced secondary materials n_{tnre} are allocated to the fabrication of recycled products with an allocation parameter ϵ_{pn}. The material allocation is only a distribution process; no losses are considered at this stage. The fabrication yield λ_p determines the final products produced from allocated secondary materials m_{tpne}. The product-specific fabrication yields are assumed to be the same for secondary materials as for primary materials. The fabrication yields are aggregate numbers including both the fabrication yield of original material input and the recovery and processing of process wastes. In analogy to the fabrication losses from primary production in the initial period, the fabrication yield also determines the fabrication stage's losses from secondary production by mass balance. The material flows of final products demanded after the initial period are determined by the material composition of allocated scrap, the remelting yield, the material allocation parameter, and the fabrication yield:

$$x_{tpne} = \lambda_p \ \epsilon_{pn} \sum_{r} \sum_{s} \rho_{nre} w_{trse}\,. \tag{4}$$

MaTrace-multi runs iteratively, 1 year after each other. Details on the mass balance equations and parameter choices of each process depicted in Figure 1 are shown in Supporting Information S1. Formally, MaTrace-multi is a special case of MaTrace-alloy (Nakamura et al., 2017) with two types of alloys: designed (strictly controlled) alloys made of primary metals m and unintentional (not strictly controlled) alloys made of end-of-life scraps n. Accordingly, mixing of m and n occurs in the waste sorting processes where materials M are converted into scrap s as well as in the allocation of scraps to remelting processes r. The statistical composition of secondary materials depends on the composition of products produced as cohorts in preceding years, taking the elemental composition of preceding secondary materials into consideration. The actual elemental composition of future secondary materials will be a superimposition of different cohorts' statistical compositions. Here, we only calculate the 1000-year fate of elements from the final demand for products made from primary materials.

Materials can be circulated and used if they are not dissipated in any of the processes. Six dissipative losses are considered: mining losses ℓ^m, fabrication losses ℓ^f, in-use dissipation ℓ^u, collection losses ℓ^c, sorting losses ℓ^s, and remelting losses ℓ^r. Each of these dissipative losses is calculated from the corresponding process's mass balance, explained in detail in Supporting Information S1. The total dissipation is calculated by $\ell = \ell^m + \ell^f + \ell^u + \ell^c + \ell^s + \ell^r$.

All calculations are implemented using the open software framework *ODYM*, which keeps track of the modeled processes and flows in the material flow system, the classifications for all indices used, and provides a standard format for parameter sheets (Pauliuk & Heeren, 2020). The ODYM-MaTrace-multi script in python (v3.9.4), the configuration and classification files, all parameters, and the key calculated flows, stocks, and indicators (all provided in spreadsheet format) are included in the accompanying OSF repository (Helbig et al., 2021).

2.3 | Key indicators

To evaluate the effectiveness of the waste management and open-loop recycling system, we use two key indicators: The circularity and the longevity of each metal, as defined by Klose and Pauliuk (2021). The circularity describes how often a metal is used or reused. The quantified value is a statistical mean of the number of product use-phases that the atoms of a metal cohort experience before they dissipate. Some atoms will not enter any product lifetime because they are already lost during primary production. In contrast, some atoms may be used many times because they enter the use-phase of a product with high collection and recycling rates again and again. However, in theory, the circularity does not tell us about the decay rate of in-use stocks because the secondary materials may well be used only in short-lived products. The circularity of metal e in the material flow system is calculated by the following equation:

$$\mathrm{CIRC}_e = \frac{\sum_t \sum_p \sum_M x_{tpMe}}{\sum_t e_{te}} = \frac{\sum_t \sum_p \sum_M x_{tpMe}}{\sum_t \ell_{te}}. \tag{5}$$

The second equality holds only approximately in numerical calculations, and convergence is achieved with a long time horizon.

Longevity describes the time span of a metal in the anthroposphere. The quantified value is a statistical mean of the total time span between extraction from the lithosphere and any form of dissipation for a metal cohort's atoms. Some atoms will be immediately dissipated during primary production; therefore, their time span in the anthroposphere is negligible. In contrast, some atoms provide service in products or infrastructure for a long time or through multiple life cycles. The longevity of metal *e* in the material flow system is calculated by the following equations, which hold if the time horizon is long enough:

$$\mathrm{LONG}_e = \frac{\sum_t t\,\ell_{te}}{\sum_t \ell_{te}} = \frac{\sum_t \sum_p \sum_M S_{tpMe}}{\sum_t \ell_{te}}. \tag{6}$$

The denominator $\sum_t \ell_{te}$ can be replaced with $\sum_t e_{te}$, as the approximation shown in Equation (5). In an ideal circular economy, metals would be used for long times, resulting in a high value for longevity, and multiple times, resulting in a high value for circularity. We can estimate the progress toward a circular economy for each of the metals with these two indicators, calculated from a joint model. Note that Klose and Pauliuk (2021) defined both circularity and longevity using the initial stocks as the denominator, not on the extraction or the losses because they started their calculation with the first use-phase instead of the extraction from lithosphere (see Section 2.11 in Supporting Information S1).

In the base case, the circularity and longevity indicators do not differentiate between functional and non-functional recycling; they only quantify the fate of metals in open-loop recycling. It may very well be that recycled chemical elements serve no purpose in the secondary material, for example, nickel and chromium in carbon steel, which are tolerated but lose the functionality they provide in stainless steel. Even worse are contaminants like copper in stainless steel, which need to be held below tolerance levels to prevent adverse effects on material properties. The details of calculating circularity and longevity under consideration of non-functional recycling either with a binary functionality matrix or with the embodied energy information, are explained in Table S1 in Supporting Information S1.

2.4 | Monte Carlo simulation

We run the model multiple times with exogenous parameters subject to different uncertainty distributions. For each parameter, one of three different levels of variance was chosen and applied with the beta or Dirichlet distributions depending on the parameter properties. Details on calculating the uncertainty distributions and the Monte Carlo simulation are explained in Supporting Information S1.

3 | RESULTS

Total stocks for the seven metals are in the magnitude of teragrams (Tg) in SI units, or in more familiar terms, megatons (Mt). Flows are in gigagrams (Gg) or kilotons (kt). For example, the model traces 805 Mt of iron and 1.48 Mt nickel. These masses are based on the necessary extraction from the lithosphere to provide the primary materials contained in the initial final demand, as calculated with the WIO-MFA methodology. The values are somewhat smaller than the USGS mining production estimations for 2011, which is partly caused by the selection of the 11 EXIOBASE3 product categories and the consideration of only the final demand for these categories instead of the whole economy; see Table S1 in Supporting Information S1. In the beginning, this total mass for each metal comprises mining losses, initial fabrication losses, and initial in-use stocks. The initial in-use stocks of each metal in each end-use sector is calculated from the mass of the final products demanded and their initial material composition. The model results can be summarized with stock dynamics, flow dynamics, and circularity and longevity.

3.1 | Stock dynamics

Total in-use stocks for all metals decline over time by definition and are virtually diminished by the end of the 1000 years. Still, the in-use stock of individual product categories may increase for some time after the initial period. In contrast, cumulative dissipative losses increase over time. The sum of total in-use stock and cumulative dissipative losses is unchanged for all years and all metals because of the mass balance. Figure 2 shows the dynamics of in-use stocks and dissipative losses of all seven metals for the first two centuries. High-resolution figures for each subplot of the metals and the result data for all 1000 years are available in Supporting Information S1.

Aluminum shows an underlying pattern of gradually changing from stocks of wrought aluminum to cast aluminum. This transition explains why initially, the construction sector is the most extensive aluminum application, increasing from 12.1 to 14.0 Mt in the first 20 years. Still, after 45 years, the in-use stock in the construction sector falls behind the in-use stock in motor vehicles at a level of 8.7 Mt. After 100 years, 10.3 (4.1 to 20.0) Mt

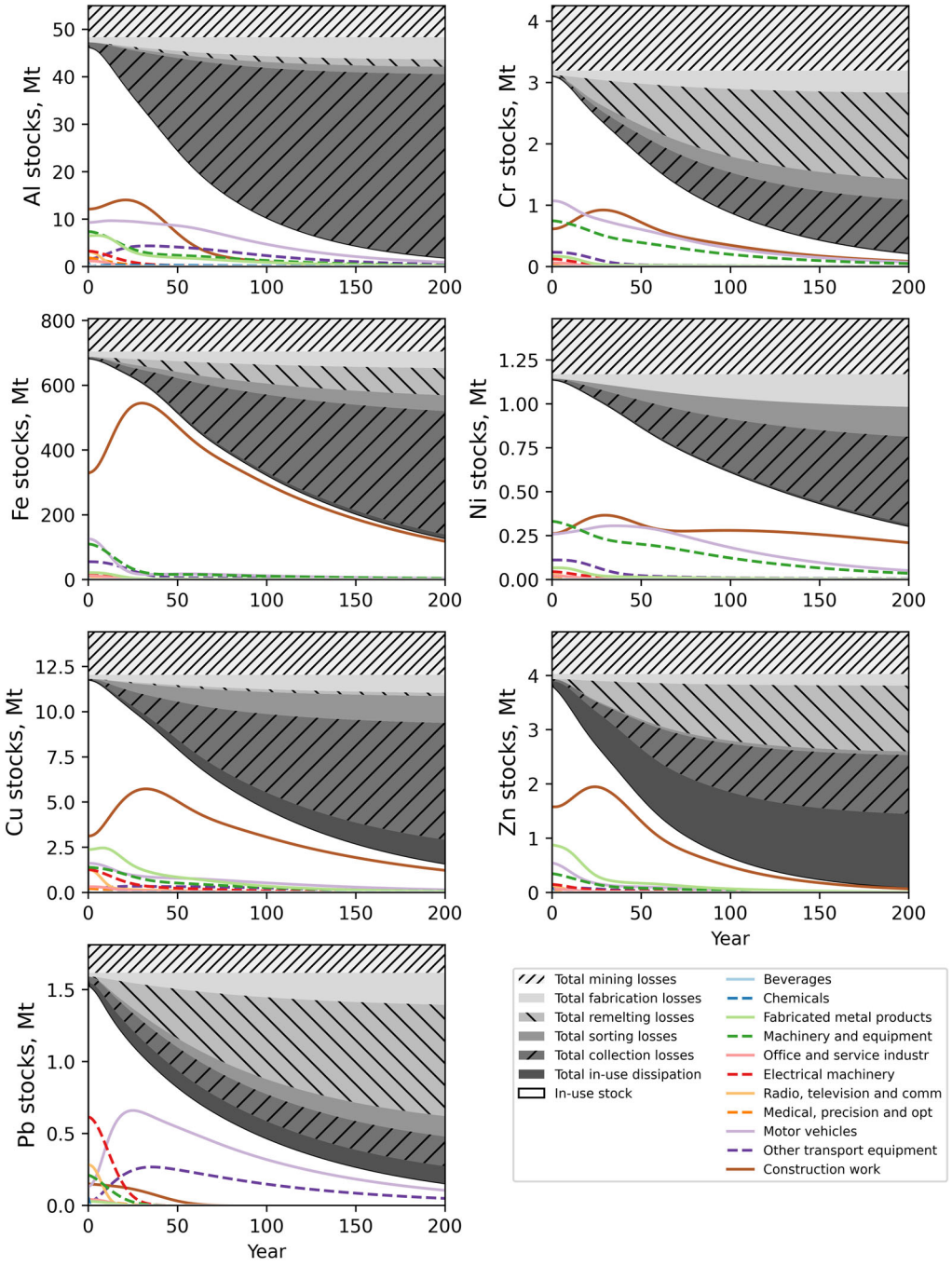

FIGURE 2 Fate of initial metal stocks of aluminum, chromium, iron, nickel, copper, zinc, and lead over the first two centuries. The stacked area plot shows the total remaining in-use stocks and the different cumulative dissipative losses. Line plots break down the total in-use stock into end-use product categories. The white-colored part represents "in-use stock." Underlying data for Figure 2 are available in Supporting Information S2

remain as total in-use stock, where the numbers in parentheses represent the interval from the 2.5 percentile to 97.5 percentile obtained from the Monte Carlo simulation. Seventy-three percent of the dissipative losses of Al occur as collection losses.

Chromium is unique among the seven metals insofar as there is no dedicated remelting process to produce secondary chromium. Instead, chromium gets recycled as steel, either through carbon steel remelting or stainless steel remelting. In the beginning, more chromium is contained in motor vehicles and machinery and equipment than in the construction sector. Because of the allocation of recycled steel, however, the in-use stocks of chromium in the construction sector rise to about one-and-a-half times the initial stock and peak 29 years after the start of the simulation. After 100 years, 885 (564 to 1305) kt remain as total in-use stock. Of all dissipative losses of Cr, 36% occur as remelting losses.

Iron already starts with about half of its in-use stock in the construction sector, which rapidly increases because recycled steel is mainly used in the construction sector. Therefore, the in-use stock in construction increases from 328 to 544 Mt over the first 30 years, while the total in-use stock decreases from 687 to 608 Mt in the same time frame. The construction sector primarily determines iron's stock dynamics and its steel types by this time. After 100 years, 323 (200 to 450) Mt remain as total in-use stock. Collection losses are most important for Fe, representing 59% of all dissipative losses.

In the case of nickel, the short-term recycling pattern differs from the long-term recycling pattern. While the recycling of nickel products as nickel matte recycling contributes to the first decades of the simulation, this contribution becomes negligible. The recycling then happens mostly through austenitic stainless steel remelting. In the beginning, machinery contains most of the primary nickel with 330 kt, but this gradually shifts to motor vehicles and the construction sector, almost equal after 60 years with 280 kt in-use stock. Afterward, all in-use stocks decline, but the decay is slowest once again for the construction sector. After 100 years, 612 (420 to 786) kt remain as total in-use stock. Forty-nine percent of the dissipative losses of Ni occur as collection losses.

Copper also shows a substantial shift over time toward in-uses stocks in the construction sector, almost doubling the initial stock in this sector within 30 years. After 100 years, 4.62 (2.88 to 6.40) Mt remain as total in-use stock. Fifty-three percent of the dissipative losses of Cu occur as collection losses.

Within the analyzed seven metals, zinc has the highest share of in-use dissipative losses. Twenty-nine percent of all dissipative losses are because of in-use dissipation. The second-highest percentage for in-use dissipation is calculated for copper with 11%. This strong in-use dissipation is one reason why zinc shows the lowest circularity and longevity in this study. Despite starting with about three times as much primary production, the in-use stocks of zinc after 100 years are similar to nickel, with 649 (356 to 965) kt still in use. Collection losses are responsible for 23% of zinc's dissipative losses, and remelting losses make up 26%.

The specialty of lead is that recycled lead is predominantly used in automotive batteries. Therefore, there is a shift from electrical machinery to motor vehicles in the in-use stock in the first 25 years. During this time, the in-use stock in motor vehicles increases from 129 to 659 kt, whereas the in-use stock of electrical machinery decreases from 614 to 64 kt. After 100 years, 466 (198 to 861) kt lead remain as total in-use stock. Lead is the only metal for which remelting losses are the main source of dissipative losses with 48%.

One option for quantifying the mixing and dilution effects in open-loop recycling is the relative statistical entropy (RSE) method developed by Rechberger and Brunner (2002). If we apply this method to the stocks and total losses over the total period, we observe that despite the mixing shown in Figure 3, the vast majority of RSE stems from dilution effects. The maximum statistical entropy, H_{max}, would be reached if all traced material were dispersed into the environmental background concentration. In year 60, the contribution of mixing of elements has the highest statistical entropy with 0.6% of H_{max} or 1.5% of the RSE in that year. Overall, the RSE is increasing and asymptotically reaches H_{max} at the end of the period, because most of the stock is lost to the environment; see Figure S1 in Supporting Information S1.

3.2 | Flow dynamics

Next to the stock dynamics, *MaTrace-multi* also allows the analysis of flow dynamics. It is crucial to keep in mind that these are statistical material flows of just one cohort of primary material extracted from the lithosphere in 1 year to meet the final demand of that initial year and traced over time. Therefore, the elemental content does not represent the total chemical composition in a future year. However, it does show how elements are cycled as a statistical average and, therefore, allows tracing the fate in open-loop recycling.

Sankey diagrams are a suitable display to show where precisely mixing and potential contamination happens within the material cycle. Figure 3 shows the material flows for all seven metals in sorted scrap, allocated scrap, remelted secondary materials, sorting losses, and remelting losses 30 years after the initial period. Individual Sankey diagrams for year 30 and combined Sankey diagrams for years 10, 50, and 100 are shown in Supporting Information S1. In total, 14.0 Mt is collected 30 years after the initial period. The most significant part of this is iron, making up 11.8 Mt of the Sankey diagram's material flows. The second is aluminum with 1.54 Mt. All other metals combined only contribute 636 kt of the collected end-of-life waste in that year.

In the sorting process, two observations of the model can be made. The first is that 30 years after the initial period, many metals exit their first use-phase. Therefore, they are still collected in this model as primary materials *m*. This importance of primary materials can be observed particularly for iron with a large share of long-lifetime applications. In contrast, there is already a more significant flow of secondary cast aluminum waste than primary aluminum waste. The second observation is that there are several wrong sorting cases, which leads to, for example, aluminum elements being mistakenly identified as steel scrap or pieces of iron entering the aluminum scrap flows.

The second stage shows the allocation of scrap types to different types of remelting processes. In this stage, sorted and identified wrought aluminum nevertheless gets used in the cast aluminum refining process. One can also see that both galvanized steel scrap, which is carbon steel with a zinc coating, and carbon steel scrap, are used in the carbon steel remelting process. There is no dedicated galvanized steel remelting process. Austenitic stainless steel and Ni-alloy steel scrap are also both allocated to the same remelting process.

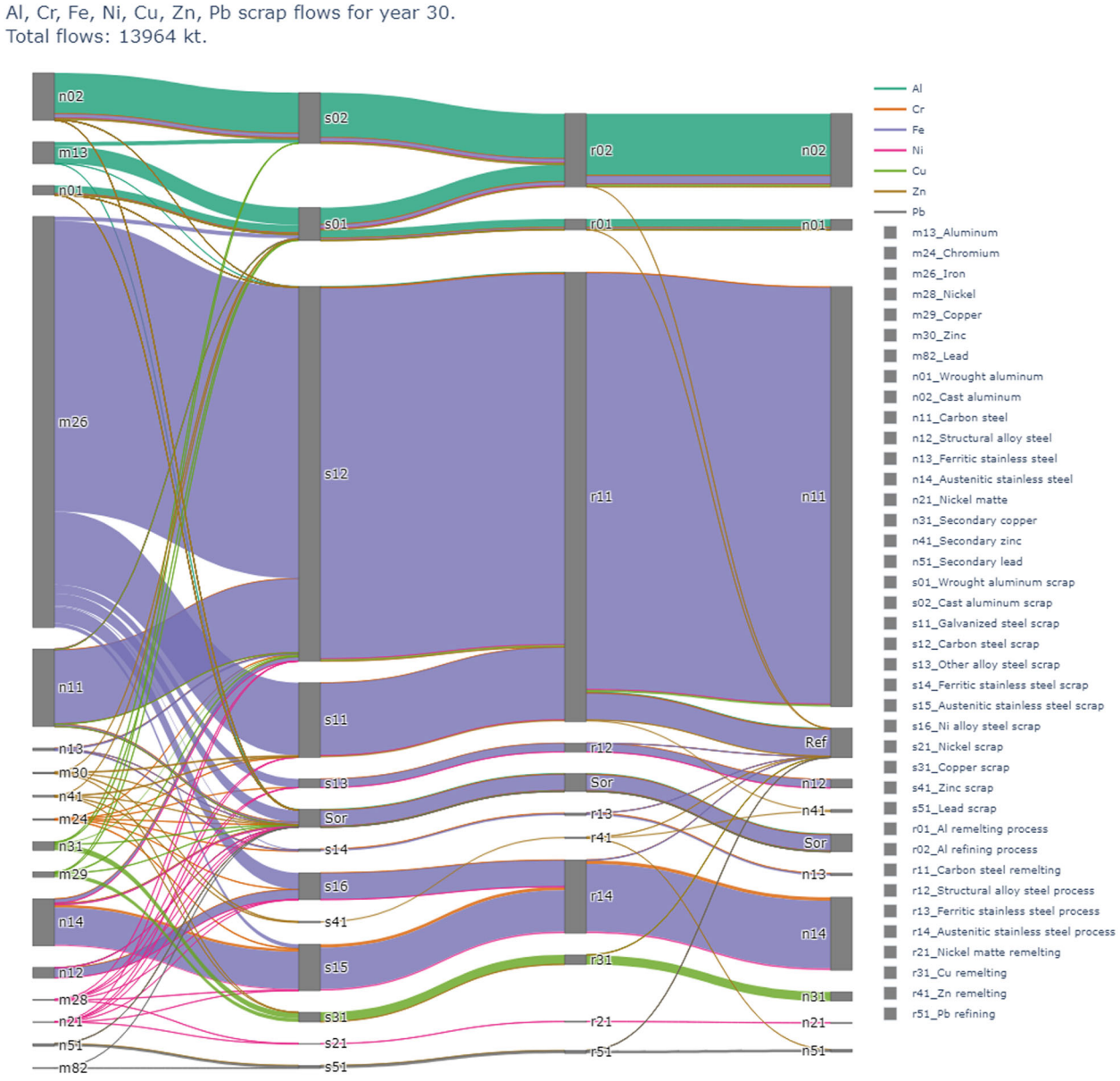

FIGURE 3 Sankey diagram for scrap and remelting flows for primary and secondary materials of Al, Cr, Fe, Ni, Cu, Zn, and Pb in year 30. Primary materials are indicated with index *m*, secondary materials with *n*, scraps with *s*, and remelting processes with *r*. Sor, sorting losses; Ref, remelting losses. Underlying data for Figure 2 are available in Supporting Information S2

The third stage is where thermodynamics comes into play. In the aluminum remelting and refining processes, only half the zinc content of scrap is removed. All other elements maintain in the secondary material, be they contaminants or desired alloying elements. For more noble elements, such as Cu, Ni, and Pb, contamination with iron or aluminum is generally removed in the electrolysis. For carbon steel remelting, a part of the vaporized zinc is recollected and becomes secondary zinc.

If we again apply the RSE method (Rechberger & Brunner, 2002) to quantify the mixing effects, but this time only on the waste management sector shown in Figure 3, and further consider a complete dilution of the end-of-life wastes occurring in each year as the maximum statistical entropy, we get the results that through the processes of waste sorting, scrap allocation, and remelting, the RSE is increased by between 6% and 9.1% of H_{max} of each year, respectively; see Figure S2 in Supporting Information S1.

3.3 | Circularity and longevity

Circularity values are lowest for zinc with 1.94 (1.52 to 2.47) applications on average and highest for nickel with 5.13 (3.46 to 8.78) applications. Longevity values are the shortest for zinc with 47 (37 to 61) years and longest for nickel with 116 (78 to 205) years. Figure 4 shows the circularity

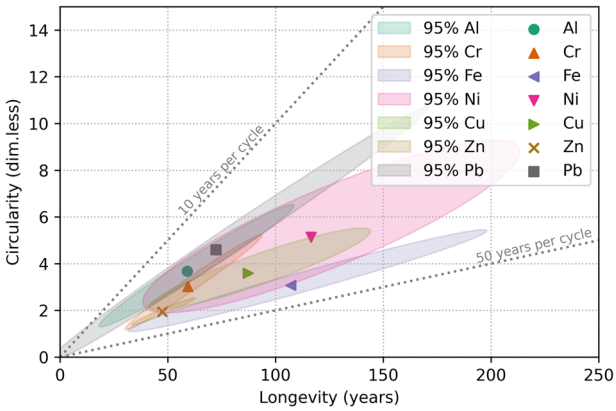

FIGURE 4 Circularity and longevity of Al, Cr, Fe, Ni, Cu, Zn, and Pb. The scatter plot shows the mean values and ellipsoids that approximate the 95% regions. The correlation between circularity and longevity is considered using the Mahalanobis distance estimated in the Monte Carlo simulation. Underlying data for Figure 2 are available in Supporting Information S2

TABLE 1 Results for longevity and circularity in the base case, in the two cases with functionality consideration (using binary service index or embodied energy), and without considering losses before the first use-phase

	LONG base case (years)	LONG with binary functionality (years)	LONG embodied energy functionality (years)	LONG w/o pre-use loss (years)
Al	59.0	59.0	59.0	68.7
Cr	59.3	46.0	53.7	80.9
Fe	107.1	105.9	107.1	125.5
Ni	116.5	67.5	78.1	151.2
Cu	87.3	44.3	55.7	106.6
Zn	47.5	47.2	47.4	58.0
Pb	72.4	72.4	72.4	82.5
	CIRC base case	**CIRC with binary functionality**	**CIRC embodied energy functionality**	**CIRC w/o pre-use loss**
Al	3.672	3.672	3.672	4.272
Cr	3.023	2.693	2.887	4.123
Fe	3.072	2.990	3.072	3.598
Ni	5.130	3.919	4.198	6.660
Cu	3.589	1.992	2.801	4.383
Zn	1.936	1.920	1.932	2.364
Pb	4.595	4.595	4.595	5.235

Note: The calculations for approximating the 95% region and the scatter plots for each of the metals from individual Monte Carlo simulation runs can be found in Supporting Information S1.

and longevity of all seven metals. We use an ellipsoid to approximate the 95% confidence region of longevity and circularity. The center of the ellipsoid is the point of averages. The radius is a minimum, say r, such that the Mahalanobis distance from the center is smaller than r for at least 95% of Monte Carlo runs (Mahalanobis, 1936; Rencher & Christensen, 2012).

The correlation between circularity and longevity in the different Monte Carlo simulation runs is very high for all metals, with correlation coefficients ranging from 0.87 for nickel to 0.99 for lead. The correlation is increased if the lifetimes of product categories to which recycled materials are allocated do not vary significantly between Monte Carlo runs. There is significant uncertainty in the nickel case whether nickel elements are recycled in Ni matte refining or stainless steel recycling. In contrast, there is only one lead recycling process. All recycled lead is allocated to motor vehicles and other transportation equipment—and the allocation between these two sectors is relatively well known.

Lead and aluminum have particularly short average lifetimes per use-phase. The ratio between longevity and circularity is 16 years on average per cycle for both metals. This ratio is the highest for iron, for which cycles last 35 years on average.

Table 1 shows how the longevity and circularity are affected by considering functionality aspects. Excluding non-functional recycling from the circularity and longevity calculations, either with binary service index or with the embodied energy information, does not change the values for Al,

Fe, Zn, and Pb significantly, if at all. For Cu, however, the longevity would be halved to just 44 years (binary functionality) and reduced significantly to 56 years (embodied energy). The circularity of Cu would be reduced to 1.99 and 2.8, respectively. For Ni, functionality consideration causes a much more substantial reduction of longevity (shortened by 42% or 33%) than circularity (reduced by 24% or 18%, respectively). Excluding the losses before the first use-phase increases longevity and circularity by between 14% for lead and 36% for chromium.

4 | DISCUSSION AND CONCLUSION

With *MaTrace-multi*, it is possible to trace the fate of seven major metals simultaneously in a planetary model for the first time. The model allows quantifying metal-specific circularity and longevity and identifying causes for dissipation throughout open-loop recycling. Simultaneously tracing seven metals allows the evaluation of material mixing through sorting and remelting processes while considering the thermodynamic realities (Reuter & Kojo, 2012). Quantifying mixing, contamination, and alloy composition is an essential but still underdeveloped aspect in industrial ecology research. This first version of the planetary multi-element model comes at the cost of lower modeling resolution. For example, to compensate for global EXIOBASE3's lower resolution with 200 product items (Stadler et al., 2018), the initial material composition of the final products demanded had to be approximated by the Japanese IO table with 619 product items (Ohno et al., 2014). This material composition is then reaggregated to the product categories of EXIOBASE3 for final products demanded, assuming the Japanese product mix applies to the global production. The material flows' chemical composition is only a statistical value, not a real scrap or alloy composition. *MaTrace-multi* traces one cohort of material extracted within 1 year—and does not replenish dissipated material flows with additional extraction. In the global socioeconomic material cycles, the flows emerging from cohorts of consecutive years overlap. Because it is a global one-region model, no information on the regional distribution of dissipative losses can be calculated.

The results highlight the need for increased end-of-life collection rates as a valuable measure for a circular economy: For Al, Fe, Ni, and Cr, collection losses are the most important dissipative flows. In the sorting processes, lowering the overall sorting losses is key and increasing the share of correctly identified material flows. Therefore, to improve the sorting rates and sorting efficiency, fostering technologies like laser-induced breakdown spectroscopy may be helpful (Noll et al., 2018; Owada et al., 2018). Cycles can also be closed by design for disassembly (Nakamura & Yamasue, 2010) and design for remanufacturing (Singhal et al., 2020). However, cycles can not only be closed but also slowed through lifetime extensions and narrowed through efficiency improvements, which are both equally viable circular economy strategies (Geissdoerfer et al., 2018). The results of *MaTrace-multi* have shown that for aluminum, there is a rapid shift of the in-use stock from wrought aluminum to cast aluminum because of the existing scrap allocation. Without cast aluminum motor blocks, the introduction of battery electric vehicles causes additional challenges to the recycling system of aluminum (Hatayama et al., 2012; Løvik et al., 2014). For steel, recycling is limited to carbon steel recycling and austenitic stainless steel recycling after 100 years.

Klose and Pauliuk (2021) have recently quantified copper's circularity with 2.1 applications on average and the longevity with 47 years. This estimate is close to the lower boundary of our calculations. However, it is not surprising that the multi-metal model has higher circularity and longevity than the single-metal model because it even considers non-intended contamination flows as in-use stocks. For steel, Pauliuk (2018) calculated a longevity of 110 to 290 years, depending on the starting application, region, and recycling scenario. Compared with the longevities calculated by Helbig et al. (2020) based on a review of static MFA models, *MaTrace-multi* estimates similar longevity for Fe, shorter longevity for Al, and more extended longevity for Cr, Ni, Cu, Zn, and Pb.

In future assessments, extending the scope of metals would be worthwhile. For example, it was impossible to calculate the tin content of final products demanded from the Japanese IO table or use any other high-resolution IO table for this purpose. The inclusion of other non-metal materials like cement, wood, or plastics would be exciting from the perspective of climate mitigation but comes with the challenge that minerals and hydrocarbons can be formed and destroyed throughout the recycling process. If data on material compositions becomes available from other sources directly, our analysis no longer has to be bounded by the resolution of available IO tables. Furthermore, it would be possible to relax the assumption that fabrication yield is not material-specific if more detailed information becomes available. Overall, the methodology of *MaTrace-multi* can be used as a tool for assessing the effectiveness of circular economy strategies (Klose & Pauliuk, 2021). The results provide an alternative material-specific view on the circularity of the global economy modeled with comprehensive economy-wide MFA models, which often do not allow such element-specific disaggregation (Haas et al., 2020). The possibility to differentiate between closed-loop and open-loop recycling within a single-metal cycle and within the whole metal sector with its cycles linked through metallurgical processes, fabrication processes, and scrap sorting is a step forward in going from qualitative evaluations to quantitative assessments.

CONFLICT OF INTEREST

The authors declare no conflict of interest.

DATA AVAILABILITY STATEMENT

The data that support the findings of this study are openly available in an OSF Registry at https://doi.org/10.17605/OSF.IO/R54C6.

ORCID

Christoph Helbig https://orcid.org/0000-0001-6709-373X

Yasushi Kondo https://orcid.org/0000-0002-6855-2691

REFERENCES

Ayres, R. U., Ayres, L. W., & Råde, I. (2002). *The life cycle of copper, Its co-products and by-products*. International Institute for Environment and Development (IIED). https://pubs.iied.org/sites/default/files/pdfs/migrate/G00740.pdf

Bertram, M., Ramkumar, S., Rechberger, H., Rombach, G., Bayliss, C., Martchek, K. J., Müller, D. B., & Liu, G. (2017). A regionally-linked, dynamic material flow modelling tool for rolled, extruded and cast aluminium products. *Resources, Conservation and Recycling*, *125*, 48–69. http://linkinghub.elsevier.com/retrieve/pii/S0921344917301520

Brunner, P. H., & Rechberger, H. (2016). *Handbook of material flow analysis* (2nd ed.). CRC Press. https://www.taylorfrancis.com/books/9781315313443

Chen, W.-Q., & Graedel, T. E. (2012). Anthropogenic cycles of the elements: A critical review. *Environmental Science & Technology*, *46*(16), 8574–8586. https://doi.org/10.1021/es3010333

Ciacci, L., Reck, B. K., Nassar, N. T., & Graedel, T. E. (2015). Lost by design. *Environmental Science & Technology*, *49*(16), 9443–9451. https://doi.org/10.1021/es505515z

Cullen, J. M., & Allwood, J. M. (2013). Mapping the global flow of aluminum: From liquid aluminum to end-use goods. *Environmental Science & Technology*, *47*(7), 3057–3064. http://pubs.acs.org/doi/abs/10.1021/es304256s

Cullen, J. M., Allwood, J. M., & Bambach, M. D. (2012). Mapping the global flow of steel: From steelmaking to end-use goods. *Environmental Science & Technology*, *46*(24), 13048–13055. http://pubs.acs.org/doi/abs/10.1021/es302433p

Daehn, K. E., Serrenho, A. C., & Allwood, J. M. (2017). How will copper contamination constrain future global steel recycling? *Environmental Science & Technology*, *51*(11), 6599–6606. http://pubs.acs.org/doi/10.1021/acs.est.7b00997

Geissdoerfer, M., Morioka, S. N., de Carvalho, M. M., & Evans, S. (2018). Business models and supply chains for the circular economy. *Journal of Cleaner Production*, *190*, 712–721. https://doi.org/10.1016/j.jclepro.2018.04.159

Glöser, S., Soulier, M., & Espinoza, L. A. T. (2013). Dynamic analysis of global copper flows: Global stocks, postconsumer material flows, recycling indicators, and uncertainty evaluation. *Environmental Science & Technology*, *47*(12), 6564–6572. https://doi.org/10.1021/Es400069b

Graedel, T. E. (2019). Material flow analysis from origin to evolution. *Environmental Science & Technology*, *53*(21), 12188–12196. https://pubs.acs.org/doi/10.1021/acs.est.9b03413

Graedel, T. E., Allwood, J. M., Birat, J.-P., Buchert, M., Hagelüken, C., Reck, B. K., Sibley, S. F., & Sonnemann, G. (2011). What do we know about metal recycling rates? *Journal of Industrial Ecology*, *15*(3), 355–366. https://doi.org/10.1111/j.1530-9290.2011.00342.x

Graedel, T. E., van Beers, D., Bertram, M., Fuse, K., Gordon, R. B., Gritsinin, A., Harper, E. M., Kapur, A., Klee, R. J., Lifset, R., Memon, L., & Spatari, S. (2005). The multilevel cycle of anthropogenic zinc. *Environmental Science & Technology*, *9*(3), 67–90. https://doi.org/10.1162/1088198054821573

Haas, W., Krausmann, F., Wiedenhofer, D., Lauk, C., & Mayer, A. (2020). Spaceship earth's odyssey to a circular economy: A century long perspective. *Resources, Conservation and Recycling*, *163*, 105076. https://doi.org/10.1016/j.resconrec.2020.105076

Hatayama, H., Daigo, I., Matsuno, Y., & Adachi, Y. (2012). Evolution of aluminum recycling initiated by the introduction of next-generation vehicles and scrap sorting technology. *Resources, Conservation and Recycling*, *66*, 8–14. https://doi.org/10.1016/j.resconrec.2012.06.006

Helbig, C., Thorenz, A., & Tuma, A. (2020). Quantitative assessment of dissipative losses of 18 metals. *Resources, Conservation and Recycling*, *153*, 104537. https://doi.org/10.1016/j.resconrec.2019.104537

Helbig, C., Kondo, Y., & Nakamura, S. (2021). ODYM-MaTrace-multi. OSF, September 24. osf.io/r54c6.

Izatt, R. M., Izatt, S. R., Bruening, R. L., Izatt, N. E., & Moyer, B. A. (2014). Challenges to achievement of metal sustainability in our high-tech society. *Chemical Society Reviews*, *43*(8), 2451. https://doi.org/10.1039/c3cs60440c

Jelinski, L. W., Graedel, T. E., Laudise, R. A., McCall, D. W., & Patel, C. K. (1992). Industrial ecology: Concepts and approaches. *Proceedings of the National Academy of Sciences*, *89*(3), 793–797. http://www.pnas.org/cgi/doi/10.1073/pnas.89.3.793

Johansson, N., & Krook, J. (2021). How to handle the policy conflict between resource circulation and hazardous substances in the use of waste? *Journal of Industrial Ecology*, *25*(4), 994–1008. https://onlinelibrary.wiley.com/doi/10.1111/jiec.13103

Johnson, J., Schewel, L., & Graedel, T. E. (2006). The contemporary anthropogenic chromium cycle. *Environmental Science & Technology*, *40*(22), 7060–7069. https://pubs.acs.org/doi/10.1021/es060061i

Klose, S., & Pauliuk, S. (2021). Quantifying longevity and circularity of copper for different resource efficiency policies at the material and product levels. *Journal of Industrial Ecology*, *25*(4), 979–993. https://onlinelibrary.wiley.com/doi/10.1111/jiec.13092

Krausmann, F., Wiedenhofer, D., Lauk, C., Haas, W., Tanikawa, H., Fishman, T., Miatto, A., Schandl, H., & Haberl, H. (2017). Global socioeconomic material stocks rise 23-fold over the 20th century and require half of annual resource use. *Proceedings of the National Academy of Sciences*, *114*(8), 1880–1885. http://www.pnas.org/lookup/doi/10.1073/pnas.1613773114

Lamb, W. F., Wiedmann, T., Pongratz, J., Andrew, R., Crippa, M., Olivier, J. G. J., Wiedenhofer, D., Mattioli, G., Al Khourdajie, A., Pachauri, S., Figueroa, M., Shaeb, Y., Slade, R., Hubacek, K., Sun, L., Ribeiro, S. K., Khennas, S., du Can S. de la R., Chapungu, L., Davis, S. J., Bashmakov, I., Dai, H., Dhakal, S., Tan, X., Geng, Y., Gu, B., & Minx, J. (2021). A review of trends and drivers of greenhouse gas emissions by sector from 1990 to 2018. *Environmental Research Letters*, *16*(7), 073005. https://iopscience.iop.org/article/10.1088/1748-9326/abee4e

Lèbre, É., Corder, G., & Golev, A. (2017). The role of the mining industry in a circular economy: A framework for resource management at the mine site level. *Journal of Industrial Ecology*, *21*(3), 662–672. https://doi.org/10.1111/jiec.12596

León, M. F. G., Blengini, G. A., & Dewulf, J. (2020). Cobalt in end-of-life products in the EU, where does it end up: The MaTrace approach. *Resources, Conservation and Recycling*, *158*, 104842. https://doi.org/10.1016/j.resconrec.2020.104842

Løvik, A. N., Modaresi, R., & Müller, D. B. (2014). Long-term strategies for increased recycling of automotive aluminum and its alloying elements. *Environmental Science & Technology*, *48*(8), 4257–4265. http://pubs.acs.org/doi/abs/10.1021/es405604g

Mahalanobis, P. C. (1936). On the general distance in statistics. *Proceedings of the National Institute of Sciences of India*, *2*(1), 49–55.

Mao, J., Dong, J., & Graedel, T. E. (2008a). The multilevel cycle of anthropogenic lead: I. Methodology. *Resources, Conservation and Recycling*, *52*(8–9), 1058–1064. https://doi.org/10.1016/j.resconrec.2008.04.004

Mao, J., Dong, J., & Graedel, T. E. (2008b). The multilevel cycle of anthropogenic lead. II. Results and discussion. *Resources, Conservation and Recycling*, *52*(8–9), 1050–1057. https://doi.org/10.1016/j.resconrec.2008.04.005

Meylan, G., & Reck, B. K. (2017). The anthropogenic cycle of zinc: Status quo and perspectives. *Resources, Conservation and Recycling*, *123*, 1–10. http://linkinghub.elsevier.com/retrieve/pii/S0921344916300064

Müller, E., Hilty, L. M., Widmer, R., Schluep, M., & Faulstich, M. (2014). Modeling metal stocks and flows: A review of dynamic material flow analysis methods. *Environmental Science & Technology*, *48*(4), 2102–2113. https://doi.org/10.1021/Es403506a

Nakajima, K., Matsubae-Yokoyama, K., Nakamura, S., Itoh, S., & Nagasaka, T. (2008). Substance flow analysis of zinc associated with iron and steel cycle in Japan, and environmental assessment of EAF dust recycling process. *ISIJ International*, *48*(10), 1478–1483. http://joi.jlc.jst.go.jp/JST.JSTAGE/isijinternational/48.1478?from=CrossRef

Nakajima, K., Takeda, O., Miki, T., Matsubae, K., Nakamura, S., & Nagasaka, T. (2010). Thermodynamic analysis of contamination by alloying elements in aluminum recycling. *Environmental Science & Technology*, *44*(14), 5594–5600. http://pubs.acs.org/doi/abs/10.1021/es9038769

Nakamura, S., Kondo, Y., Kagawa, S., Matsubae, K., Nakajima, K., & Nagasaka, T. (2014). MaTrace: Tracing the fate of materials over time and across products in open-loop recycling. *Environmental Science & Technology*, *48*(13), 7207–7214. http://pubs.acs.org/doi/abs/10.1021/es500820h

Nakamura, S., Kondo, Y., Nakajima, K., Ohno, H., & Pauliuk, S. (2017). Quantifying recycling and losses of Cr and Ni in steel throughout multiple life cycles using MaTrace-alloy. *Environmental Science & Technology*, *51*(17), 9469–9476. http://pubs.acs.org/doi/abs/10.1021/acs.est.7b01683

Nakamura, S., Nakajima, K., Kondo, Y., & Nagasaka, T. (2007). The waste input-output approach to materials flow analysis. *Journal of Industrial Ecology*, *11*(4), 50–63. https://doi.org/10.1162/jiec.2007.1290

Nakamura, S., & Yamasue, E. (2010). Hybrid LCA of a design for disassembly technology: Active disassembling fasteners of hydrogen storage alloys for home appliances. *Environmental Science & Technology*, *44*(12), 4402–4408. https://pubs.acs.org/doi/10.1021/es903340h

Noll, R., Fricke-Begemann, C., Connemann, S., Meinhardt, C., & Sturm, V. (2018). LIBS analyses for industrial applications—An overview of developments from 2014 to 2018. *Journal of Analytical Atomic Spectrometry*, *33*(6), 945–956.

Nuss, P., & Eckelman, M. J. (2014). Life cycle assessment of metals: A scientific synthesis. *PLoS ONE*, *9*(7), e101298. https://doi.org/10.1371/journal.pone.0101298

Ohno, H., Matsubae, K., Nakajima, K., Nakamura, S., & Nagasaka, T. (2014). Unintentional flow of alloying elements in steel during recycling of end-of-life vehicles. *Journal of Industrial Ecology*, *18*(2), 242–253. https://doi.org/10.1111/jiec.12095

Owada, S., Suzuki, R., Kamata, Y., & Nakamura, T. (2018). Novel pretreatment process of critical metals bearing e-scrap by using electric pulse disintegration. *Journal of Sustainable Metallurgy*, *4*(2), 157–162. https://doi.org/10.1007/s40831-018-0170-8

Pauliuk, S. (2018). Critical appraisal of the circular economy standard BS 8001:2017 and a dashboard of quantitative system indicators for its implementation in organizations. *Resources, Conservation and Recycling*, *129*, 81–92. https://doi.org/10.1016/j.resconrec.2017.10.019

Pauliuk, S., & Heeren, N. (2020). ODYM—An open software framework for studying dynamic material systems: Principles, implementation, and data structures. *Journal of Industrial Ecology*, *24*(3), 446–458. https://onlinelibrary.wiley.com/doi/abs/10.1111/jiec.12952

Pauliuk, S., Kondo, Y., Nakamura, S., & Nakajima, K. (2017). Regional distribution and losses of end-of-life steel throughout multiple product life cycles—Insights from the global multiregional MaTrace model. *Resources, Conservation and Recycling*, *116*, 84–93. http://linkinghub.elsevier.com/retrieve/pii/S0921344916302774

Puype, F., Samsonek, J., Knoop, J., Egelkraut-Holtus, M., & Ortlieb, M. (2015). Evidence of waste electrical and electronic equipment (WEEE) relevant substances in polymeric food-contact articles sold on the European market. *Food Additives and Contaminants: Part A*, *32*(3), 410–426. https://doi.org/10.1080/19440049.2015.1009499

Rechberger, H., & Brunner, P. H. (2002). A new, entropy based method to support waste and resource management decisions. *Environmental Science & Technology*, *36*(4), 809–816. https://doi.org/10.1021/Es010030h

Reck, B. K., & Graedel, T. E. (2012). Challenges in metal recycling. *Science*, *337*(6095), 690–695. https://doi.org/10.1126/science.1217501

Reck, B. K., Müller, D. B., Rostkowski, K., & Graedel, T. E. (2008). Anthropogenic nickel cycle: Insights into use, trade, and recycling. *Environmental Science & Technology*, *42*(9), 3394–3400. https://pubs.acs.org/doi/10.1021/es072108l

Reck, B. K., & Rotter, V. S. (2012). Comparing growth rates of nickel and stainless steel use in the early 2000s. *Journal of Industrial Ecology*, *16*(4), 518–528. https://doi.org/10.1111/j.1530-9290.2012.00499.x

Rencher, A. C., & Christensen, W. F. (2012). *Methods of multivariate analysis* (3rd ed.). Wiley.

Reuter, M. A., Heiskanen, K., Boin, U., van Schaik, A., Verhoef, E. V., Yang, Y., & Georgalli, G. (2005). *The metrics of material and metal ecology*. Elsevier.

Reuter, M. A., & Kojo, I. V. (2012). Challenges of metals recycling. *Materia*, *2*(2012), 50–57.

Reuter, M. A., van Schaik, A., & Ballester, M. (2018). Limits of the circular economy: Fairphone modular design pushing the limits. *World of Metallurgy - ERZMET-ALL*, *71*(2), 68–79. https://www.scopus.com/inward/record.uri?eid=2-s2.0-85046467167&partnerID=40&md5=b8db3bce1a068ccbdee1cf8aa73af5ee

Reuter, M. A., van Schaik, A., Gutzmer, J., Bartie, N., & Abadías-Llamas, A. (2019). Challenges of the circular economy: A material, metallurgical, and product design perspective. *Annual Review of Materials Research*, *49*(1), 253–274. https://www.annualreviews.org/doi/10.1146/annurev-matsci-070218-010057

Singhal, D., Tripathy, S., & Jena, S. K. (2020). Remanufacturing for the circular economy: Study and evaluation of critical factors. *Resources, Conservation and Recycling*, *156*, 104681. https://doi.org/10.1016/j.resconrec.2020.104681

Stadler, K., Wood, R., Bulavskaya, T., Södersten, C.-J., Simas, M., Schmidt, S., Usubiaga, A., Acosta-Fernández, J., Kuenen, J., Bruckner, M., Giljum, S., Lutter, S., Merciai, S., Schmidt, J. H., Theurl, M. C., Plutzar, C., Kastner, T., Eisenmenger, N., Erb, K.-H., de Koning, A., Tukker, A. (2018). EXIOBASE 3: Developing a time series of detailed environmentally extended multi-regional input-output tables. *Journal of Industrial Ecology*, *22*(3), 502–515. https://doi.org/10.1111/jiec.12715

Turner, A., & Filella, M. (2017). Field-portable-XRF reveals the ubiquity of antimony in plastic consumer products. *Science of The Total Environment*, *584–585*: 982–989. https://doi.org/10.1016/j.scitotenv.2017.01.149

Van der Voet, E., van Oers, L., Verboon, M., & Kuipers, K. (2019). Environmental implications of future demand scenarios for metals: Methodology and application to the case of seven major metals. *Journal of Industrial Ecology*, *23*(1), 141–155.

Wang, T., Müller, D. B., & Graedel, T. E. (2007). Forging the anthropogenic iron cycle. *Environmental Science & Technology*, *41*(14), 5120–5129. https://pubs.acs.org/doi/10.1021/es062761t

Watari, T., Nansai, K., Giurco, D., Nakajima, K., McLellan, B., & Helbig, C. (2020). Global metal use targets in line with climate goals. *Environmental Science & Technology*, *54*(19), 12476–12483. https://pubs.acs.org/doi/10.1021/acs.est.0c02471

Zimmermann, T., & Gößling-Reisemann, S. (2013). Critical materials and dissipative losses: A screening study. *Science of The Total Environment*, *461-462*, 774–780. http://linkinghub.elsevier.com/retrieve/pii/S0048969713005834

SUPPORTING INFORMATION

Additional supporting information may be found in the online version of the article at the publisher's website.

How to cite this article: Helbig C, Kondo Y, Nakamura S. Simultaneously tracing the fate of seven metals at a global level with MaTrace-multi. *J Ind Ecol*. 2022;*26*:923–936. https://doi.org/10.1111/jiec.13219